

Available online at www.sciencedirect.com

SCIENCE @ DIRECT®

JOURNAL OF **CRYSTAL
GROWTH**

Journal of Crystal Growth ■ (■■■■) ■■■-■■■

www.elsevier.com/locate/jcrysgr

Multiple stationary solutions of an irradiated slab

P.D. Taylor*, D.L. Feltham

*Centre for Polar Observation and Modelling, Department of Space and Climate Physics, University College London,
Gower Street, London WC1E 6BT, UK*

Received 10 August 2004; accepted 26 November 2004

Communicated by M.E. Glicksman

Abstract

A mathematical model describing the heat budget of an irradiated medium is introduced. The one-dimensional form of the equations and boundary conditions are presented and analysed. Heat transport at one face of the slab occurs by absorption (and reflection) of an incoming beam of short-wave radiation with a fraction of this radiation penetrating into the body of the slab, a diffusive heat flux in the slab and a prescribed incoming heat flux term. The other face of the slab is immersed in its own melt and is considered to be a free surface. Here, temperature continuity is prescribed and evolution of the surface is determined by a Stefan condition. These boundary conditions are flexible enough to describe a range of situations such as a laser shining on an opaque medium, or the natural environment of polar sea ice or lake ice. A two-stream radiation model is used which replaces the simple Beer's law of radiation attenuation frequently used for semi-infinite domains. The stationary solutions of the governing equations are sought and it is found that there exists two possible stationary solutions for a given set of boundary conditions and a range of parameter choices. It is found that the existence of two stationary solutions is a direct result of the model of radiation absorption, due to its effect on the albedo of the medium. A linear stability analysis and numerical calculations indicate that where two stationary solutions exist, the solution corresponding to a larger thickness is always stable and the solution corresponding to a smaller thickness is unstable. Numerical simulations reveal that when there are two solutions, if the slab is thinner than the smaller stationary thickness it will melt completely, whereas if the slab is thicker than the smaller stationary thickness it will evolve toward the larger stationary thickness. These results indicate that other mechanisms (e.g. wave-induced agglomeration of crystals) are necessary to grow a slab from zero initial thickness in the parameter regime that yields two stationary solutions.

© 2004 Elsevier B.V. All rights reserved.

PACS: 44.10.+i; 81.10.Fq; 91.60.Mk; 92.40.Sn

Keywords: A1. Directional solidification; A1. Heat transfer; A1. Radiation

*Corresponding author. Tel.: +44 020 7679 7378; fax: +44 020 7979 7883.

E-mail addresses: pdt@cpom.ucl.ac.uk (P.D. Taylor), dlf@cpom.ucl.ac.uk (D.L. Feltham).

1. Introduction

In this paper, we consider a one-dimensional opaque slab that is affected by external sources of radiation. The optical properties of the slab allow radiation to penetrate and cause internal heating. In this paper, we use a two-stream radiation model and analyse the stationary solutions of the one-dimensional model, comparing it to the results where the radiation is described using Beer's law. Using the two-stream radiation model, it is found that there can be two stationary solutions, which arise solely due to the variation of albedo with depth. The smaller solution is found to be unstable, also because of the depth dependence of albedo.

In Section 2, the mathematical model of the heat budget of an irradiated slab is described and the one-dimensional form of the governing equations is cast into nondimensional form. The choice of geometry and boundary conditions are particularly appropriate to a layer of naturally forming ice exposed to solar radiation. However, since our model and results are quite general, we have decided to present the problem in less specific terms. The statement of the stationary problem is presented in Section 3, where the stationary temperature profile is given and the equation defining the stationary slab thickness is given. In Section 4, the stationary problem is solved using specific choices of the parameters and surface heat fluxes. Plots of the loci of stationary depth as incident fluxes are varied are presented and contrasted with those that arise when using Beer's law. In Section 5, a linear stability analysis is performed that shows that when there are two stationary solutions, the smaller thickness solution is unstable. Numerical simulations reveal that if the slab is thinner than the smaller stationary thickness it will melt completely, whereas if the slab is thicker than the smaller stationary thickness it will evolve toward that larger stationary thickness. Finally, in Section 6, our main conclusions are restated and discussed.

2. Mathematical formulation

We consider a homogeneous slab of infinite horizontal extent with one face exposed to an

incoming beam of radiation propagating through a medium of low optical density, which we shall denote short-wave radiation, and the other face immersed in its own melt and considered to be a free surface. The geometry and boundary conditions are illustrated in Fig. 1 and describe, for example, a layer of ice floating on a lake exposed to solar radiation. The co-ordinate system has its origin at the exposed face of the slab, with the z -axis pointing toward the face immersed in melt. The thickness of the slab is denoted by h .

Local conservation of energy within the slab is given by

$$\rho c \frac{\partial T}{\partial t} = k \frac{\partial^2 T}{\partial z^2} - \frac{\partial F_{\text{net}}(z; h)}{\partial z}, \quad (1)$$

where $T(z, t)$ is the local temperature. The volumetric specific heat capacity of the slab is given by ρc and k is the thermal conductivity. The final term in the heat balance, $F_{\text{net}}(z; h)$, is the net irradiance at a point inside the slab, and it is assumed that all attenuation of short-wave radiation inside the slab is converted to heat. The equation for conservation of energy (1) shows the rate of change of temperature within a control volume at fixed position (first term), due to thermal diffusion (second term) and internal heating (third term).

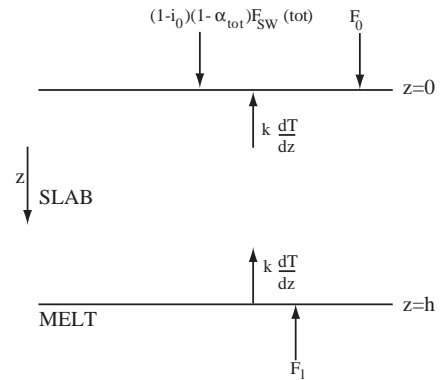


Fig. 1. Slab of infinite horizontal extent with one face exposed to short-wave radiation and the other face immersed in its own melt. The surface fluxes are described in the text.

We consider the boundary condition at the exposed face of the slab to be given by

$$k \frac{\partial T}{\partial z} + (1 - i_0)(1 - \alpha_{\text{tot}})F_{\text{SW}}(\text{tot}) + F_0 = 0 \quad (z = 0), \quad (2)$$

where i_0 parameterises the amount of incoming short-wave energy that passes through this surface of the slab and is distinguishable from other energy sources at the surface, α_{tot} is the total albedo of the slab, $F_{\text{SW}}(\text{tot})$ is the total incoming short-wave irradiance at the surface, and F_0 represents other sources of energy at the surface, such as outgoing long-wave radiation, latent heat of evaporation or sublimation and incoming long-wave radiation. Eq. (2) states that at the exposed face of the slab there is a balance between the conductive flux from the slab (first term), the net short-wave radiation at the surface (second term), and other energy sources (third term).

The face of the slab immersed in its own melt is a free surface and thus there are two boundary conditions there. The temperature at the slab–melt boundary is continuous and we take this temperature to be equal to the melting temperature of the slab T_m ; therefore

$$T = T_m \quad (z = h). \quad (3)$$

The position of the free boundary is determined from the Stefan condition

$$\rho \mathcal{L} \frac{dh}{dt} = k \frac{\partial T}{\partial z} - F_1 \quad (z = h), \quad (4)$$

where F_1 is the heat flux directed from the melt into the slab. Eq. (4) balances the rate of latent heat released/absorbed upon freezing or melting (first term) to the diffusive energy flux into the slab (second term) and the energy flux from the melt (third term).

The two-stream radiation model calculates the up-welling and down-welling irradiances in a medium. The irradiance into (out of) a plane at a given wavelength is defined to be the radiance projected onto a plane and integrated over the hemisphere above (below) the plane, and has units $\text{W m}^{-2} \text{nm}^{-1}$. The net irradiance at a point is the difference between the down-welling and up-welling irradiances. The specific type of two-stream

model used in this paper has been used previously in polar research (e.g. Refs. [1,2]). A simple exponential decay of down-welling irradiance with depth of penetration into an optically dense medium and zero up-welling irradiance (Beer's law) emerges as a special case of the two-stream radiation model either when there is no scattering or when the depth of the slab is infinite. An advantage of the two-stream radiation model is that the albedo is calculated in terms of optical scattering and absorption characteristics. Using Beer's law, the albedo must be prescribed.

The equations that describe the variation with depth of up-welling (F_\uparrow) and down-welling (F_\downarrow) irradiance for the two-stream model are

$$\frac{\partial F_\downarrow}{\partial z} = -(k^* + r^*)F_\downarrow^j + r^*F_\uparrow \quad (5)$$

and

$$\frac{\partial F_\uparrow}{\partial z} = (k^* + r^*)F_\uparrow - r^*F_\downarrow, \quad (6)$$

where k^* and r^* are the absorption and scattering coefficients, respectively. Eq. (5) describes the change in the down-welling irradiance (first term) because of loss due to absorption and scattering of the down-welling stream (second and third terms) and gain due to scattering of the up-welling stream (fourth term). Eq. (6) describes the change in the up-welling irradiance (first term) because of loss due to absorption and scattering of the up-welling stream (second and third terms) and gain due to scattering of the down-welling stream (fourth term).

The general solution of Eqs. (5) and (6) under the restriction that $r^* \neq 0$ is

$$F_\downarrow = sAe^{\kappa z} + \frac{B}{s}e^{-\kappa z} \quad (7)$$

and

$$F_\uparrow = Ae^{\kappa z} + Be^{-\kappa z}, \quad (8)$$

where $s = (\kappa - k^*)/(\kappa + k^*)$, $\kappa = k^{*2} + 2k^*r^*$ is the extinction coefficient, and A and B are optical coefficients dependent upon optical properties and thickness.

The boundary condition for the radiation model applied to the slab face exposed to incoming,

short-wave radiation is

$$F_{\downarrow} = R_0 F_{\uparrow} + (1 - R_0) i_0 F_{\text{SW}} \quad (z = 0), \quad (9)$$

where R_0 is the coefficient of Fresnel reflection (reflection due to differences in the real part of the index of refraction between the slab and optically less dense medium), i_0 is the fraction of incident radiation that is not absorbed at the surface of the slab, and F_{SW} is the incident short-wave irradiance at a particular wavelength. Eq. (9) states that the down-welling irradiance at the surface (first term) is given by the reflected component of the up-welling irradiance at the surface (second term) plus the penetrating component of the incoming short-wave irradiance (third term).

We assume that the melt does not scatter any incident radiation back into the slab; thus

$$F_{\uparrow} = 0 \quad (z = h). \quad (10)$$

Given the boundary conditions (Eqs. (9) and (10)), the optical coefficients are found to be

$$A = \frac{F_{\text{SW}} i_0 (1 - R_0) s}{s^2 + R_0 s \{-1 + \exp(2\kappa h)\} - \exp(2\kappa h)} \quad (11)$$

and

$$B = -\frac{F_{\text{SW}} i_0 (1 - R_0) s \exp(2\kappa h)}{s^2 + R_0 s \{-1 + \exp(2\kappa h)\} - \exp(2\kappa h)}. \quad (12)$$

In the limit $h \rightarrow \infty$, $A \rightarrow 0$ and the coefficient B becomes

$$B_{\infty} = \frac{F_{\text{SW}} i_0 (1 - R_0) s}{1 - R_0 s}, \quad (13)$$

which results in Beer's law (exponential decay of net irradiance).

The total net irradiance is given by

$$F_{\text{net}}(z; h) = (F_{\downarrow} - F_{\uparrow}) A, \quad (14)$$

where A is the bandwidth of the incident radiation, so that $F_{\text{SW}}(\text{tot}) = F_{\text{SW}} A$.

The proportion of incoming short-wave radiation reflected at the surface over the waveband A

(the spectral albedo) is

$$\begin{aligned} \alpha &= R_0 + (1 - R_0) \frac{F_{\uparrow}}{F_{\text{SW}}} \\ &= \frac{[R_0 + s\{i_0(1 - R_0)^2 - R_0^2\}]}{(1 - R_0 s) - \exp(-2\kappa h)s(s - R_0)} \\ &\quad - \frac{\exp(-2\kappa h)s[i_0(1 - R_0)^2 + R_0(s - R_0)]}{(1 - R_0 s) - \exp(-2\kappa h)s(s - R_0)}, \end{aligned}$$

which is identical to the total albedo α_{tot} (the spectrally weighted albedo) since we only consider a single band of radiation.

We now nondimensionalise our model equations with a typical lengthscale L , a thermal diffusive timescale $L^2 \rho c / k$, and a short-wave radiative scale F . The nondimensional temperature θ is given by

$$\theta = \frac{T - T_m}{\Delta T}, \quad (15)$$

where $\Delta T = 1.2 \text{ K}$ is a typical temperature difference across the slab. The dimensionless melting temperature of the slab, equal to the lower boundary temperature, is $\theta = 0$.

The nondimensional problem is

$$\frac{\partial \theta}{\partial t} = \frac{\partial^2 \theta}{\partial z^2} - \mathcal{F} \frac{\partial F_{\text{net}}(z; h)}{\partial z}, \quad (16)$$

$$\begin{aligned} \frac{\partial \theta}{\partial z} + \mathcal{F}(1 - i_0)(1 - \alpha_{\text{tot}}) F_{\text{SW}}(\text{tot}) \\ + \mathcal{F} F_0 = 0 \quad (z = 0), \end{aligned} \quad (17)$$

$$\theta = 0 \quad (z = h), \quad (18)$$

and

$$\mathcal{S} \frac{dh}{dt} = \frac{\partial \theta}{\partial z} - \mathcal{F} F_1 \quad (z = h). \quad (19)$$

The dimensionless parameters are the Stefan number

$$\mathcal{S} = \frac{\mathcal{L}}{c \Delta T}, \quad (20)$$

and the ratio of the short-wave radiative scale to the typical conductive heat flux through the slab

$$\mathcal{F} = \frac{FL}{k \Delta T}. \quad (21)$$

3. Definition of the stationary problem

The solution(s) of a system of differential equations and boundary conditions that are independent of time (i.e. all time derivatives are zero) are known as stationary solution(s). A *stable* stationary solution will typically represent the state of a system subjected to constant or slowly varying boundary conditions. In terms of our irradiated slab model, we require several conditions to be met for a stationary solution to be physically realisable: we require that the thickness is real and positive ($h \in \mathfrak{R}^+$); that the temperature within the slab does not exceed the melting temperature and is above absolute zero (θ_0), so that $\theta_0 < \theta \leq 0$; and that the stationary solution is stable to infinitesimal perturbations (i.e. it is linearly stable). If a stationary solution is linearly unstable, then it will not be observed in reality.

The stationary problem is given by the stationary form of the heat balance equation inside the slab

$$\frac{\partial^2 \theta}{\partial z^2} - \mathcal{F} \frac{\partial F_{\text{net}}(z; h)}{\partial z} = 0, \quad (22)$$

the boundary conditions (17) and (18), and the stationary form of the Stefan condition

$$\frac{\partial \theta}{\partial z} - \mathcal{F} F_1 = 0 \quad (z = h). \quad (23)$$

The stationary solution(s) of this problem are the pair $\{\theta^{\text{ss}}(z), h^{\text{ss}}\}$, where $\theta = \theta^{\text{ss}}(z)$ is the stationary temperature profile in the slab and $h = h^{\text{ss}}$ is the stationary slab thickness.

Integration of the stationary heat balance (22) from h to z , using the stationary Stefan condition (23), yields

$$\frac{\partial \theta}{\partial z} = g(z), \quad (24)$$

where

$$g(z) = \mathcal{F} F_{\text{net}}(z; h) - \mathcal{F} F_{\text{net}}(h; h) + \mathcal{F} F_1. \quad (25)$$

Eqs. (24) and (25) show that no stationary solutions exist for this model when $F_1 < 0$, since otherwise $\partial \theta / \partial z < 0$ at $z = h$ implying that there would be internally molten regions of the slab. Eq. (24) subject to boundary condition (18)

has solution

$$\theta(z) = \mathcal{F} \left(\int_h^z F_{\text{net}}(z'; h) dz' + (F_1 - F_{\text{net}}(h; h))(z - h) \right). \quad (26)$$

Application of the final boundary condition (17) now shows that the stationary slab depth is determined solely by the radiation model and the incident heat fluxes given by

$$F_{\text{net}}(0; h) - F_{\text{net}}(h; h) + (1 - i_0)(1 - \alpha_{\text{tot}})F_{\text{SW}}(\text{tot}) = \Gamma, \quad (27)$$

where

$$\Gamma = -F_1 - F_0 \quad (28)$$

is the total energy flux lost by the slab to its surroundings. Eq. (27) is simply an expression of global conservation of energy, which states that the total energy flux gained through absorption of short-wave radiation at the upper surface and in the interior of the slab (left-hand side) is equal to the total energy flux lost at the boundaries of the slab (right-hand side).

4. Solution of the stationary equations

The stationary problem formulated in the preceding section is now solved. There are ranges of parameter values in which there are two stationary solutions. The sensitivity of the results to variations in boundary conditions is also presented. These are compared to results that are obtained when the radiation model is replaced by Beer's law, determined by taking the limit of the two-stream radiation model as the thickness tends to infinity.

Substituting for irradiances, the thickness equation (27) may be written directly as a quadratic in exponentials:

$$A^* e^{2\kappa L h} + B^* e^{\kappa L h} + C^* = 0, \quad (29)$$

where

$$A^* = \Gamma(1 - R_0 s) - F_{\text{SW}}(\text{tot})(1 - R_0) \times (1 + (-R_0 + i_0(-2 + i_0 + R_0))s), \quad (30)$$

Table 1
Parameter values used for a single band of short-wave irradiance

$F_{\text{SW}}(\text{tot}) = 1$	$s = 0.7$	$\kappa = 1.5 \text{ m}^{-1}$	$i_0 = 0.7$	$R_0 = 0.05$
$F_1 = 0.025$	$F_0 = -0.275$	$\mathcal{F} = 83.33$	$\Delta T = 1.2 \text{ K}$	$L = 1 \text{ m}$

$$B^* = F_{\text{SW}}(\text{tot})i_0(1 - R_0)(1 - s^2), \quad (31)$$

and

$$C^* = -\Gamma s(s - R_0) + F_{\text{SW}}(\text{tot})s(1 - R_0) \times (-R_0 + i_0(-2 + i_0 + R_0) + s). \quad (32)$$

Eq. (29) is straight-forwardly solved to yield two potential solutions given by

$$h^{\text{ss}} = \frac{1}{\kappa L} \log \left(\frac{-B^* \pm \sqrt{B^{*2} - 4A^*C^*}}{2A^*} \right). \quad (33)$$

For a physically real thickness, we require that $h = h^{\text{ss}} > 0$, which implies that $e^{\kappa L h^{\text{ss}}} > 1$. Given an arbitrary quadratic equation of the form $A^*x^2 + B^*x + C^* = 0$, with $B^* > 0$ and real solutions x_1 and x_2 , it is straightforward to show [3] that the conditions for both $x_1 > 1$ and $x_2 > 1$ are

$$A^* < 0, \quad (34)$$

$$2A^* + B^* > 0, \quad (35)$$

and

$$A^* + B^* + C^* < 0. \quad (36)$$

By definition $B^* > 0$ and using Eqs. (30)–(32) it may be shown that these conditions are equivalent to

$$\Gamma < F_{\text{SW}}(\text{tot})X, \quad (37)$$

$$\Gamma > F_{\text{SW}}(\text{tot})Y, \quad (38)$$

and

$$\Gamma < F_{\text{SW}}(\text{tot})Z, \quad (39)$$

respectively, where

$$X = \frac{(1 - R_0)(1 + (-R_0 + i_0(-2 + i_0 + R_0))s)}{(1 - R_0s)}, \quad (40)$$

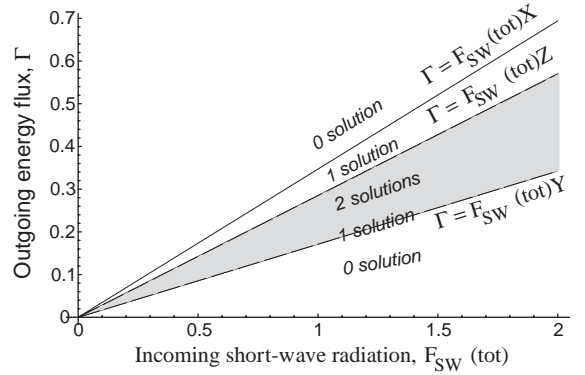


Fig. 2. Diagram to show the range of outgoing energy fluxes from the slab Γ for a given short-wave flux $F_{\text{SW}}(\text{tot})$, for which there are two stationary solutions (shaded grey). The three lines are the boundaries of the inequalities (37)–(39) that determine the number of stationary solutions. Also shown are the number of solutions possible in other areas of the domain.

Y

$$= \frac{(1 - R_0)(2 - i_0 + 2(-R_0 + i_0(-2 + i_0 + R_0))s + i_0s^2)}{2(1 - R_0s)}, \quad (41)$$

and

$$Z = (1 - i_0)(1 - R_0). \quad (42)$$

The relative positions of the lines $\Gamma = XF_{\text{SW}}(\text{tot})$, $\Gamma = YF_{\text{SW}}(\text{tot})$, and $\Gamma = ZF_{\text{SW}}(\text{tot})$ in an $F_{\text{SW}}(\text{tot})$ - Γ plot determine the number of solutions. For values given in Table 1, the three lines are plotted in Fig. 2 and the region for which there can be two real and positive solutions is shaded grey. Also indicated in the plot are the number of solutions in other regions. The parameters given in Table 1 correspond approximately to the physical properties of ice and the incident heat fluxes and short-wave radiation correspond to those found at high latitudes during spring.

This contrasts with the result obtained if Beer's law is used. In this case the thickness equation is

simply a linear function of exponentials and has at most one solution given by

$$h^{ss} = -\frac{1}{\kappa L} \log \left[1 - \left(\frac{\Gamma - (1 - i_0)(1 - \alpha_{tot})F_{SW}(tot)}{(1/s - 1)B_\infty} \right) \right]. \quad (43)$$

For Beer's law, the requirement that $h^{ss} > 0$ leads to the condition that $\Gamma - (1 - i_0)(1 - \alpha_{tot})F_{SW}(tot) > 0$, since the denominator in the solution is positive, which is simply stating that to ensure the slab does not melt completely the slab must be losing energy overall to its surroundings faster than it is gaining radiative energy at its upper surface.

The reason for the difference in behaviour between the two-stream radiation model and Beer's law is most clearly elucidated by examining the solutions from a geometrical perspective. Fig. 3 shows both sides of the thickness equation (27) as a function of the slab depth for both the two-stream radiation model and Beer's law. The right-hand side of the equation Γ , the total energy flux leaving the slab, is a constant and is shown by the solid horizontal line in the figure. The two other solid curves in the figure represent the left-hand

side of the equation, i.e. the short-wave energy absorbed by the slab at the surface and in the interior of the slab. The two-stream radiation model yields the curve that has a turning point, whereas Beer's law yields the monotonic curve. Solutions of the equation are given by the intersection of these curves with the solid horizontal line. Clearly, the two-stream solution has two stationary thicknesses and Beer's law has just one, for the parameters that are used (see Table 1), indicated by the vertical dashed lines. The sole reason that there are potentially two solutions when the two-stream radiation model is used is because of the dependence of albedo on the depth of the slab. If the albedo were independent of depth, then only one solution of Eq. (27) is possible as the energy absorbed within the interior of the slab ($F_{net}(0; h) - F_{net}(h; h)$) is a monotonic increasing function of slab thickness for any type of radiation model in this situation. Therefore, there can never be more than one stationary solution when the albedo is independent of depth.

Fig. 3 also shows the physical interpretation of the parameters used to deduce when there can be two physically real solutions for the two-stream model (Eqs. (37)–(39)). The parameter $F_{SW}(tot)X$ represents the value of the absorbed incoming short-wave energy (left-hand side of Eq. (27)) in the case of infinite depth, $F_{SW}(tot)Z$ represents the value of the absorbed incoming short-wave energy in the case of zero depth, and $F_{SW}(tot)Y$ represents the value of the absorbed incoming short-wave energy at the thickness at which there is a turning point.

For the parameters given in Table 1, the two stationary solutions for the two-stream radiation model have thicknesses 0.090 and 0.534, and for Beer's law the stationary thickness is 0.456. The temperature profiles within the slab for the three different solutions are shown in Fig. 4. The larger thickness solutions (two-stream and Beer's law) absorb more radiation near their surfaces, which leads to increased conductive heat flux within the interior of the slab in our stationary solution. The smaller thickness solution (two-stream) is not absorbing much energy since it is thin, even though the reduced albedo means that the irradiance is greater within the slab in this case compared to the larger solutions.

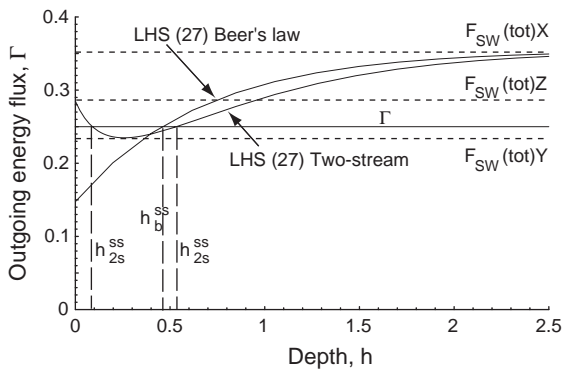


Fig. 3. Diagram showing the stationary slab thicknesses for Beer's law and the two-stream radiation model. Solutions are given by the intersections of the left-hand side of Eq. (27) with the solid horizontal line (net outgoing heat flux), and are indicated by the vertical dashed lines. Subscript 2s implies the two-stream model, and subscript b implies Beer's law. The horizontal dashed lines are the particular values of the left-hand side of Eq. (27) which dictate how many solutions there can be for a given value of Γ . These are given explicitly by Eqs. (40)–(42).

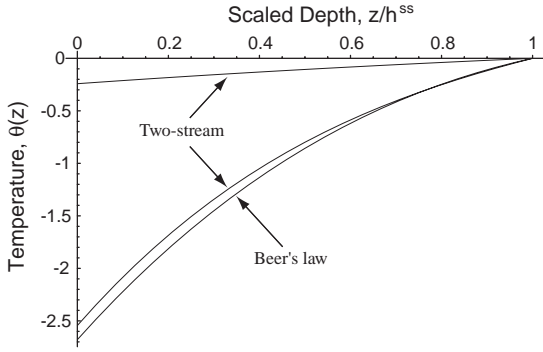


Fig. 4. Temperature profiles within a slab for two-stream solutions and Beer's law solution determined using parameters from Table 1. The thicknesses of the two-stream solutions are 0.090 and 0.534, and the thickness of the Beer's law solution is 0.456 in non-dimensional units.

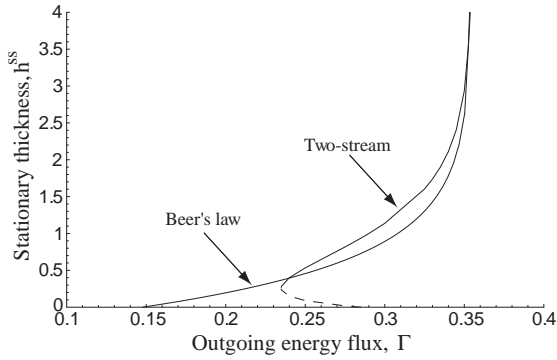


Fig. 5. Variation of stationary slab thickness h^{ss} with non-dimensional incoming flux Γ . Using the parameters in Table 1.

We calculated the variation of stationary slab thickness with variation in the boundary fluxes. Figs. 5 and 6 show the variation of the stationary thickness h^{ss} as Γ and $F_{SW}(\text{tot})$ are independently varied, holding all the other parameters fixed. For each figure there is a significant range for which there exist two stationary slab thicknesses for the same forcing data. There are also regions where only one solution or no solutions exist.

5. Linear stability analysis of stationary solutions

In order for the stationary solutions to be physically realisable, they must be linearly stable.

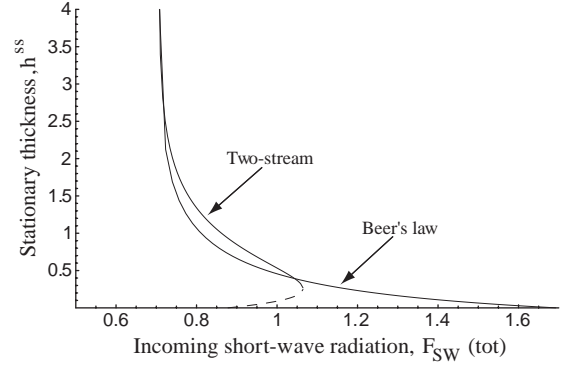


Fig. 6. Variation of stationary slab thickness h^{ss} with non-dimensional incoming shortwave flux $F_{SW}(\text{tot})$. Using the parameters in Table 1.

We present a linear stability analysis of the stationary solutions.

Infinitesimal perturbations of normal form are considered to the stationary solution $\{\theta^{ss}(z; h^{ss}), h^{ss}\}$,

$$\theta = \theta^{ss}(z; h^{ss}) + \hat{\theta}(z; h^{ss})e^{\eta t}, \quad (44)$$

$$h = h^{ss} + \hat{h}e^{\eta t}, \quad (45)$$

where $\hat{\theta}$ and \hat{h} are the initial amplitudes of the perturbations (assumed to be small) and η is the initial growth rate of the perturbations and in general may be complex.

Upon substitution of the perturbed solution into the time-dependent equations and boundary conditions (16)–(19), using Taylor series expansions about the stationary slab thickness, neglecting products of small terms and eliminating the stationary solution, we obtain

$$\eta \hat{\theta} = \frac{\partial^2 \hat{\theta}}{\partial z^2}, \quad (46)$$

$$\hat{h} \frac{\partial^2 \theta^{ss}}{\partial z \partial h} + \frac{\partial \hat{\theta}}{\partial z} = \mathcal{F}(1 - i_0) F_{SW} \hat{h} \frac{\partial \alpha_{\text{tot}}}{\partial h} \quad (z = 0), \quad (47)$$

and

$$\hat{\theta} = 0, \quad \mathcal{L} \eta \hat{h} = \frac{\partial \hat{\theta}}{\partial z} \quad (z = h^{ss}), \quad (48)$$

where we have used the fact that

$$\frac{\partial \theta^{ss}}{\partial z} + \frac{\partial \theta^{ss}}{\partial h} = 0 \quad (z = h) \quad (49)$$

and

$$\frac{\partial^2 \theta^{ss}}{\partial z^2} + \frac{\partial^2 \theta^{ss}}{\partial z \partial h} = 0 \quad (z = h), \quad (50)$$

which are determined by differentiation of Eq. (26) and evaluation at $z = h$.

Since the perturbation temperature evolution equation is diffusive, and the boundary conditions are independent of time, we expect a direct, i.e. nonoscillating, instability so that η is anticipated to be real. The perturbation temperature can be found in closed form to be

$$\hat{\theta}(z) = \mathcal{S} \hat{h} \sqrt{\eta} \sinh(\sqrt{\eta}(z - h^{ss})) \quad (51)$$

and the growth rate is determined by substitution of this temperature perturbation solution into Eq. (47) and solving numerically for η . A secant method was used to solve for η and the growth rates were found to align along the real axis as anticipated (we are interested only in the most positive growth rate for a given stationary thickness). For example, for the parameters given in Table 1 where there were two physically real stationary solutions with thicknesses 0.090 and 0.534, the (most positive) growth rates are $\eta = 0.28$ and $\eta = -0.102$, respectively (in nondimensional units of inverse time). This process was automated and the stability of the stationary solutions calculated as the incoming short-wave flux and outgoing energy Γ was varied. This revealed that the lower branch of stationary solutions, corresponding to the thinner solutions, in Figs. 5 and 6 was unstable (dashed line), and the upper branch, corresponding to thicker solutions, and the region with only one solution, was stable (solid line). We also determined the stability of the stationary solutions for Beer's law. The stability equations remain the same as for the two-stream case, except that by definition $\partial \alpha_{tot} / \partial h$ is zero. This revealed that all physically real stationary solutions using Beer's law are stable.

The fully time-dependent equations describing the irradiated slab (16)–(19) were solved numerically using a nonlinear parabolic partial differen-

tial equation solver, D03PCF, from the Numerical Algorithms Group [3]. Running the model from a variety of initial conditions allowed the linear stability results to be compared to the full model. Initial temperature profiles were taken to be linear.

When there are two stationary solutions, it was found that for all initial thicknesses greater than the smaller stationary thickness, the slab grows or melts so as to obtain the larger stationary thickness (agreeing to within 3 decimal places of accuracy with the thickness obtained by solving the stationary solution equations separately). For initial thicknesses less than or equal to the smaller thickness, the slab melts entirely. When there is only one stationary solution, the slab always grows or melts toward the stationary thickness, and when there are no stationary solutions the slab always melts entirely.

6. Discussion and concluding remarks

The one-dimensional forms of the equations describing the heat budget of an irradiated slab were presented and the stationary solutions of the governing system of equations analysed. When the two-stream radiation model was used, the equation determining the stationary thickness was shown to be of quadratic form, clearly showing the potential for two stationary solutions to exist. The use of a more simple radiation model such as an exponential decay law for the internal irradiance (Beer's law), which does not allow variation of the albedo with thickness, cannot lead to multiple stationary solutions. This is because the two solutions are due to the nonmonotonic variation of absorbed incoming short-wave radiation with thickness (left-hand side of Eq. (27)). Beer's radiation law leads to the absorbed incoming short-wave radiation being monotonic increasing with thickness, allowing for at most one possible stationary solution, as is clearly visible in Fig. 3.

If a more sophisticated representation of the radiation were used inside the slab, such as the discrete ordinates method (e.g. Ref. [4]), it is expected that multiple stationary solutions would persist. This is because it is the gross features of the

radiation model, namely the increase of albedo with thickness, that are responsible for the multiple solutions. We would expect that a more sophisticated representation of radiation would lead to only quantitatively different results.

The stability analysis of the case with a two-stream, short-wave radiation scheme revealed that the larger stationary thickness was stable, whereas the smaller stationary thickness was unstable. Results from a numerical simulation using the full time-dependent model yielded the same results and indicated the domain of attraction for the stable states, revealing that in the case of two stationary solutions all initial thicknesses greater than the smaller stationary thickness evolve to the larger stationary thickness. For one stationary solution, all initial thicknesses evolve to the single stationary thickness, and for no stationary solutions, all initial thicknesses, melt completely or grow without bound.

The stability of the stationary solutions of the slab using the two-stream radiation model and the trajectories of the time-dependent numerical simulations are straightforwardly explained by the dependence of albedo on thickness. The albedo increases monotonically and convexly with thickness from a minimum value to a limiting value. If a perturbation to the smaller thickness stationary solution results in an increase in thickness, the albedo increases, reducing the short-wave energy absorbed in the slab, and leads to the slab thickness evolving toward the larger stationary thickness. Conversely, if a perturbation to the smaller thickness stationary solution results in a decrease in thickness, the albedo decreases, increasing the short-wave energy absorbed in the slab, and leads to the slab melting completely. Perturbations to the larger stationary thickness solution result in only small perturbations to the incoming short-wave energy (dictated by the albedo).

In contrast to this, with Beer's law it was found that all physically realisable stationary solutions were stable. This has significant implications for

the initial formation of a layer of ice, for example. If Beer's law were adopted then, provided the incoming short-wave (solar) energy is sufficiently small that there is a stationary solution, ice could form simply by freezing at the surface of a lake in the form of a slab. If the two-stream radiation model were adopted, which is more realistic than Beer's law, and the short-wave radiation were such that there were two stationary solutions, it would not be possible to grow ice directly from the surface in this manner and another mechanism would be required to produce a layer of ice thicker than the smaller stationary ice thickness. Such a mechanism could be the accumulation of tiny ice crystals that form in a supercooled body of water (frazil ice) into a layer of sufficient thickness, and indeed this is typically observed to be the case.

In low and mid latitudes there is significant diurnal variation of the incoming short-wave radiation so that it is likely that during part of the day the incoming short-wave radiation would be sufficiently weak that there is only one stationary solution, and the ice could form as a slab directly from zero initial thickness. In high latitudes, however, diurnal variation is diminished. During the Arctic/Austral spring and summer, the incident short-wave radiation is sufficiently large that there are two stationary solutions and the formation of an ice layer may be affected by the unstable smaller thickness solution described in this paper.

References

- [1] D.K. Perovich, Theoretical estimates of light reflection and transmission by spatially complex and temporally varying sea ice covers, *J. Geophys. Res.* 95 (C6) (1990) 9557–9567.
- [2] D.K. Perovich, A theoretical model of ultraviolet light transmission through Antarctic sea ice, *J. Geophys. Res.* 98 (C12) (1993) 22579–22587.
- [3] P.D. Taylor, Mathematical modelling the formation and evolution of melt ponds on sea ice, Ph.D. Thesis, University of London, 2003.
- [4] S. Chandrasekhar, *Radiative Transfer*, Oxford University Press, Oxford, 1950.